

# Adsorption of Silane onto Cellulose Fibers. II. The Effect of pH on Silane Hydrolysis, Condensation, and Adsorption Behavior

Ramzi Bel-Hassen,<sup>1</sup> Sami Boufi,<sup>1</sup> Marie-Christine Brochier Salon,<sup>2</sup> Makki Abdelmouleh,<sup>1</sup>  
Mohamed Naceur Belgacem<sup>2</sup>

<sup>1</sup>LMSE, Faculté des sciences de Sfax, BP 802-3018 Sfax, Tunisia

<sup>2</sup>LGP2, Ecole Française de Papeterie et des Industries Graphiques (INPG), BP 65, Domaine Universitaire,  
F-38402 St Martin d'Hères, France

Received 21 May 2007; accepted 14 August 2007

DOI 10.1002/app.27488

Published online 1 February 2008 in Wiley InterScience (www.interscience.wiley.com).

**ABSTRACT:** The hydrolysis of four alkoxy silane agents,  $\gamma$ -methacryloxypropyl trimethoxysilane (MPS),  $\gamma$ -mercaptopropyl trimethoxysilane (MRPS), octyl trimethoxysilane (OS), and *N*-phenyl- $\gamma$ -aminopropyl trimethoxysilane (PAPS), was carried out in an ethanol/water (80/20) solution under both acid and basic conditions. <sup>1</sup>H, <sup>13</sup>C, and <sup>29</sup>Si NMR spectroscopy were used to provide quantitative analyses of the structural components during hydrolysis and condensation reaction. The analysis revealed that the acid-catalyzed hydrolysis of silane allows the formation of high amount of silanol groups, reduced the selfcondensation reaction among silanol groups and stabilized the propor-

tion of intermediary hydrolyzed species for several days. However, under basic condition, condensation reactions proceed as soon as the hydrolysis reaction started leading to the rapid consumption of silanol groups through self-condensation and to the growth of three-dimensional high molecular structures. The interaction of MPS and MRPS with cellulose fibers and the evolution of their surface properties were then investigated using adsorption isotherms and contact angle measurement. © 2008 Wiley Periodicals, Inc. *J Appl Polym Sci* 108: 1958–1968, 2008

**Key words:** cellulose; silane; NMR; adsorption

## INTRODUCTION

Since their emergence at the industrial level 30 years ago, organo-functional silanes found a growing interest for many industrial applications, as grafting molecules in composite materials,<sup>1–6</sup> adhesion promoters for surface modification,<sup>7</sup> crosslinking agents,<sup>8</sup> and for the mechanical reinforcement of ceramic surface.<sup>9</sup> The general structure of organo-functional silanes is  $X(\text{CH}_2)_n\text{Si}(\text{OR})_3$ , where RO is an alkoxy group and X is an organo-functional group. This particular bi-functional structure is one of the reasons which contribute to their use in such wide areas application. In fact, on a one hand, the alkoxy groups OR enable the silane to be anchored to hydroxyl groups bearing surfaces, and on another hand, the functional organic moiety X (amine, methacrylic, vinylic, etc.), bonded to silicon atom via alkyl group is able to react, or even copolymerizes with organic matrices, thus enhancing the interfacial adhesion between the two phases.<sup>9</sup> Silanes with different chemical structure are commercially available. They offer an easy choice of the right reagent for a given application.

Usually, the treatment with organo-functional silanes is carried out using a diluted water–alcohol solution in a concentration ranging from 0.5 to 3%, by weight.<sup>10,11</sup> The presence of water molecules is necessary to hydrolyze the alkoxy groups (RO—), thus generating the reactive silanol (Si—OH) function, one or more of that condense with OH-rich surfaces, or simply adsorb onto them, through hydrogen bonding.<sup>1,12</sup> Subsequent heat treatment leads to the formation of both covalent linkages with the surface and the development of a crosslinked silane film. However once hydrolyzed, the silanes constitute a rather reactive system, which evolves with time as a result of the condensation of the silanol groups with each other or with the alkoxy groups forming dimeric and oligomeric structures.<sup>1,13–15</sup> This phenomenon handicaps the adsorption of OH-bearing substrates, since the concentration of silanol groups can vanish rapidly.

The kinetics of hydrolysis and condensation reactions of the silanol groups are affected by the structure of the organic part of the silane and the reaction medium and conditions (temperature, pH, concentration, amounts of water and catalyst).<sup>1,15,16</sup> It is therefore extremely important to ascertain these consecutive and competitive reactions, to use properly these coupling agents in the context of cellulose modification.

Correspondence to: B. Sami (Sami.boufi@fss.rnu.tn).

Investigation of hydrolysis and condensation reaction of organo-functional silanes have been the object of numerous interesting studies where different spectroscopic techniques such as FTIR,<sup>17,18</sup> Raman,<sup>19</sup> and NMR<sup>20–22</sup> have been used to tailor the multitude of the reactions liable to take place and to describe their evolution as a function of time. However, most of these reports have been concerned with  $\gamma$ -glycidoxypropyl trimethoxysilane (GPS),  $\gamma$ -aminopropyl triethoxysilane (APS), and  $\gamma$ -methacryloxypropyl trimethoxysilane (MPS). To the best of our knowledge  $\gamma$ -mercaptopropyl trimethoxysilane has never been studied in this context.

In previous papers,<sup>23,24</sup> we have used <sup>1</sup>H, <sup>13</sup>C, and <sup>29</sup>Si NMR as tools to probe the different species able to be generated in ethanol–water solution and have shown that the hydrolysis of APS and that of  $\gamma$ -diethylenetriaminopropyl trimethoxysilane (TAS) were very fast and that the selfcondensation yielded the corresponding oligomeric networks. However, the hydrolysis of MPS was found to be much slower and required the use of an amine as a catalyst to boost the kinetic of hydrolysis. It was also established that while a basic pH greatly enhanced the hydrolysis of alkoxy groups, it led at the same time to high extent of selfcondensation yielding a gel-like networks, which precipitate in the form of colloidal particles upon further condensation. Likewise, in a series of paper we have shown that treatment of cellulose fibers with functional silane improved the mechanical properties of the ensuing composite materials, if the appropriate coupling agent was chosen.<sup>25,26</sup> These effects were explained in terms of the ability of the functional group borne by the silane moiety to bridge covalently with the polymeric matrix, thus increasing the fiber/matrix adhesion.

In the present work we continue our investigation regarding the solution behavior (hydrolysis and condensation reaction) of two different silane viz;  $\gamma$ -mercaptopropyl trimethoxysilane (MRPS), and  $\gamma$ -methacryloxypropyl trimethoxysilane. The<sup>26,27</sup> effects of initial concentration, pH, and the hydrolysis extent on the adsorption of this two silane on cellulose fibers are studied. With these two silane we integrate two other silane (OS and PAPS) to investigate the evolution of surface properties of the ensuing treated fibers.

## EXPERIMENTAL PART

### Materials

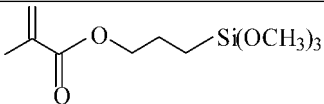
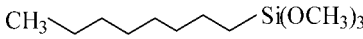
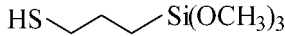
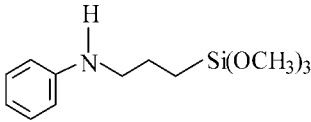
The cellulosic fibers used in this work were commercial micro-crystalline cellulose (TECHNOCEL-150DM). Their average length was about 50  $\mu$ m. The organo-functional trialkoxy silanes  $\gamma$ -methacryloxypropyl trimethoxysilane (MPS),  $\gamma$ -mercaptopropyl

trimethoxysilane (MRPS), octyl trimethoxysilane (OS), and *N*-phenyl- $\gamma$ -aminopropyl trimethoxysilane (PAPS) used to assess the kinetic behavior, were high purity products purchased from Fluka. Their structure is given in Table I. All the other reagents and solvents were commercial products of the highest purity available.

### NMR kinetics *in situ*

<sup>1</sup>H, <sup>13</sup>C, and <sup>29</sup>Si NMR spectra of the silane solutions were run on a Varian UNITY 400 spectrometer operating at 399.956, 100.572, and 79.455 MHz, respectively. All chemical shifts, relative to TMS, were measured with a coaxial insert tube containing the TMS solution as an external reference. For the <sup>1</sup>H and <sup>13</sup>C NMR, a 5-mm probe was used; the spectral widths were calibrated on the spectra to obtain the best resolution. Common 1D and 2D sequences (HMQC and HMBC) were used for a clear cut establishment of peak assignments (especially in the case of MRPS). For silicon, a 10 mm BB probe was used to optimize the signal/noise ratio for minimum acquisition times in relation with the specific reaction rates. The spectral width was 12 kHz and the relaxation delay 20 s. The proton decoupling was applied only during acquisition time to avoid negative effects. Before the data collection, all the *T*<sub>1</sub> measurements were done with the inversion-recovery

TABLE I  
The Silane Coupling Agents Used in this Work


$\gamma$ -Methacryloxypropyltrimethoxysilane MPS

octyltriméthoxysilane OS

$\gamma$ -mercaptoproyltrimethoxysilane MRPS

<i>N</i> -phenyl- $\gamma$ -aminopropylatrimethoxysilane (PAPS)

method, and the relaxation delays and the pulse widths were chosen such a way that viable quantitative spectra could be obtained. The hydrolysis and condensation reactions of the four silanes.

The kinetic studies were carried out *in situ* at 25°C in NMR tubes. The hydrolysis and condensation reactions of MRPS and MPS were carried out in a mixture of ethanol-d<sub>6</sub> and deuterated water CD<sub>3</sub>CD<sub>2</sub>OD/D<sub>2</sub>O: 80/20 (w/w) at a concentration of 10% w/w and followed *in situ* at 25°C, by recording <sup>1</sup>H, <sup>13</sup>C, and <sup>29</sup>Si NMR spectra. For alkaline conditions, TEA (2%, w/w versus solvents) was added to D<sub>2</sub>O, whereas for acidic conditions, CD<sub>3</sub>CD<sub>2</sub>OD (5%, w/w with respect to the solvent) was introduced into D<sub>2</sub>O.

### Adsorption isotherms

The adsorption isotherms were carried out at room temperature (about 25°C) adopting the following protocol: the cellulose suspension (5% w/w with respect to the solvent) in a mixture of ethanol/water 80/20 was first prepared, then appropriate amount of silane, previously dissolved in ethanol/water 80/20 solution and kept for 2–3 h to ensure the total hydrolysis of silane (in presence of acetic acid), was added. After stirring for 2 h, the cellulose fibers were then isolated by centrifugation at 2500 rpm for 20 min.

Different techniques were used to determine the quantity of adsorbed coupling agent depending on the organic function born by the silane used.

Thus, for MPS, the adsorbed amount was quantified using FTIR spectroscopy measuring the absorbency of C=O band. For this purpose well calibrated KBr pellets containing 5 mg of modified cellulose and 200 mg of KBr were prepared and the FTIR spectra recorded. For MRPS, the adsorbed quantity was determined measuring the absorbency of the residual silane by colorimetry.<sup>28</sup> Five drops of a 5,5'-dithio-bis-(2-nitrobenzoic acid) (DTNB) solution (1% wt in ethanol) were added to 5 mL of the filtrate. DTNB is a versatile water-soluble compound to quantify the free —SH groups in the solution. Thus, the addition of DTNB to free —SH containing mixture yields a yellow solution which can be quantitatively titrated by UV spectroscopy at 404 nm. Before measuring the absorbency of MRPS-DTNB solutions, their pH was adjusted to 8–9 by adding a drop of an ammonium buffer solution. It is worth noting that the extinction coefficient of DTNB is not affected by pH changes in the range of 7.6 to 8.6.<sup>29</sup>

The amount of adsorption at equilibrium  $Q_e$  (mmol g<sup>-1</sup>) was calculated as follows:

$$Q_e = \frac{(C_0 - C_e) \cdot V}{w} \quad (1)$$

where  $C_0$  and  $C_e$  (mmol L<sup>-1</sup>) are the initial and equilibrium silane concentration, respectively,  $V$  (L) the volume of the solution and  $w$  (g) the weight of cellulose sample used.

For all silanes used a calibration curve was previously built.

### Fibers characterisation

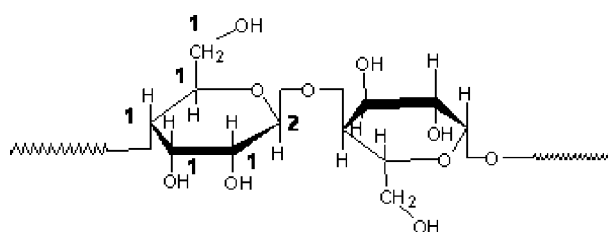
#### X-ray photoelectron spectroscopy

The used XPS spectrometer was a XSAM800 (KRATOS) operating in the fixed analyser transmission (FAT) mode, with a pass energy of 20 eV and a nonmonochromatised Al K $\alpha$  X-radiation (1486.7 eV). A current of 10 mA and a voltage of 12 kV were used. Samples were analysed in an ultra-high-vacuum (UHV) chamber ( $\sim 10^{-7}$  Pa) at room temperature, using take-off-angles (TOA) of 90° and 30° (30° allowing the analysis of thinner layer of the surface under investigation, since with such an angle, a lower depth is achieved). Samples were transferred to the XPS analysis chamber under nitrogen atmosphere. Spectra were recorded by a Sun SPARC Station 4 with Vision software (Kratos) using a step of 0.1 eV. A Shirley background was subtracted and the curve fitting for component peaks was carried out using Gaussian–Lorentzian formalism. No charge compensation (flood-gun) was used. The charge shift was corrected using the binding energy of carbon atoms bound to a hydroxyl group in cellulose,<sup>18</sup> as reference (Carbons “1” in Scheme 1). at 286.73 eV. X-ray source satellites were subtracted.

#### Contact angle

Contact angle measurements were carried out by depositing a calibrated liquid drop on the additives-free sheets of cellulose fibers (Whtman WH5). The procedure of modification of these film-like materials is similar to that reported for powdery fibers.

The contact angle apparatus used was an OCA 15 from Dataphysics, equipped with a CCD camera, with a resolution of 752 × 582 square pixels, working at an acquisition of 50 images per second. The processing of the collected data was achieved using OCA software.



**Scheme 1** Cellulose backbone structure.

**TABLE II**  
**Chemical Shifts (in ppm)  $^1\text{H}$ ,  $^{13}\text{C}$ , and  $^{29}\text{Si}$  NMR of 10% MRPS in Ethanol-d<sub>6</sub> at 25°C**

	CH <sub>2</sub> (α)	CH <sub>2</sub> (β)	CH <sub>2</sub> (γ)	OCH <sub>3</sub>	SH	Si
δ ( $^{29}\text{Si}$ )						-42.7
δ ( $^1\text{H}$ )	0.92	1.87	2.69	3.73	5.37	
δ ( $^{13}\text{C}$ )	9.24	28.78	28.17	51.16		

Cellulose substrate modification with silane was carried out by introducing it into the coupling agent solution, after 2 h of contact the sheets was recovered and dried at ambient temperature, and then it is submitted to a thermal treatment at 110°C during 2 h.

## RESULTS AND DISCUSSION

### Solution chemistry of MRPS and MPS

The peak assignments of the  $^1\text{H}$  and  $^{13}\text{C}$  NMR spectra of 10% MRPS solution in ethanol-d<sub>6</sub>, confirmed with 2D experiments, are given in Table II. We could notice that for the pristine silane the sulphur atom shield the  $\text{CH}_2(\gamma)$  carbon atom till its chemical shift is lower than that of  $\text{CH}_2(\beta)$ . Under neutral condition the hydrolysis rate of MRPS is extremely low, after 60-h reaction 5% free methanol only is released (Fig. 1). In the presence of 0.2% TEA (w/w with respect to solution) 90% hydrolysis is attained after 22 h, although in acidic medium, (i.e. with deuterated acetic acid 5% w/w with respect to the solution) after 1 h about 90% of the initial MRPS is hydrolysed. For this latter case, the  $^1\text{H}$  and  $^{13}\text{C}$  spectra display a rapid decrease of the initial MRPS  $\text{CH}_3\text{O-Si-}$  peaks at 3.73 and 51.16 ppm, respectively, and the concomitantly increase of free methanol released in solution  $\text{CH}_3\text{O-D}$  characterized by peaks at 3.51 and 49.71 ppm, respectively.

While  $^1\text{H}$  NMR is used to follow the hydrolysis kinetic by measuring the concomitant evolution of free alcohol rate in the medium and the decrease of the corresponding alkoxy group.  $^{13}\text{C}$  NMR confirms this rate, indicating that MRPS hydrolysis is much more favoured with acid catalyst than basic one.  $^{13}\text{C}$  NMR gives also some complementary information on the ratio between hydrolysis and condensation reactions. Studying  $^{13}\text{C}$  NMR spectra evolution of D<sub>2</sub>O addition MRPS under acid and basic conditions, the following remarks could be pointed out (Fig. 2):

- Under acidic conditions, there is an evolution and all the signals keep their sharp structure with peaks very well defined but at modified chemical shifts.
- On the contrary some broader signals appear and increase in presence of TEA, (solvent, free alcohol released and TEA excluded which

remain well defined). At the end of reaction the silane signals are difficultly detectable: compared with the solvent or TEA. The silane S/N seems to be drastically decreased.

- In acidic conditions there are some short lived peaks for  $\text{CH}_3\text{O}$  at the beginning of the reaction between the initial silane and the free methanol released, and the same kind of short lived entities are also noticeable for  $\text{CH}_2(\alpha)$  resonance appearing at 10, 12, and 12.9 ppm. The phenomenon is less detectable for  $\text{CH}_2(\beta)$  and  $\text{CH}_2(\gamma)$  due to their nearest chemical shifts.

As we have reported in our previous work<sup>23,24</sup> the broad signals are associated with high molecular oligomeric structures resulting from condensation reactions between silanol groups while the well defined peaks are associated with monomeric, dimeric or low molecular weight oligomeric condensed moieties.

With  $^{29}\text{Si}$  NMR more information concerning the structure of condensed species could be provided. The chemical shift of the silicon atom is function of the number of siloxane bridges. For trialkoxy silane four entities namely  $\text{T}^0$ :  $(\text{R}'\text{O})_3\text{SiR}$ ,  $\text{T}^1$ :  $(\text{R}'\text{O})_2\text{Si}(\text{OSi})\text{R}$ ,  $\text{T}^2$ :  $\text{R}'\text{OSi}(\text{OSi})_2\text{R}$  and  $\text{T}^3$ :  $\text{Si}(\text{OSi})_3\text{R}$  could be distinguished with resonance signal at (-37 to -44 ppm)  $\text{T}^0$ , (-48 to -52 ppm)  $\text{T}^1$ , (-56 to -62 ppm)  $\text{T}^2$  and (-64 to -70 ppm)  $\text{T}^3$ .<sup>30</sup> The transition from  $\text{Si-OR}'$  to the corresponding silanol  $\text{Si-OH}$  gives a shift to lower fields (because of the electron-donating properties of R') ranging from 2 up to 5 ppm according to the alkyl structure R'. The evolution of  $^{29}\text{Si}$  NMR spectra in function of time of MRPS hydrolysis in presence of acetic acid or TEA is shown on Figure 3. Some remarks could be done:

- The general overview of the silicon spectra confirm the observations done with  $^{13}\text{C}$ . In acidic media all the peaks remain well defined. With

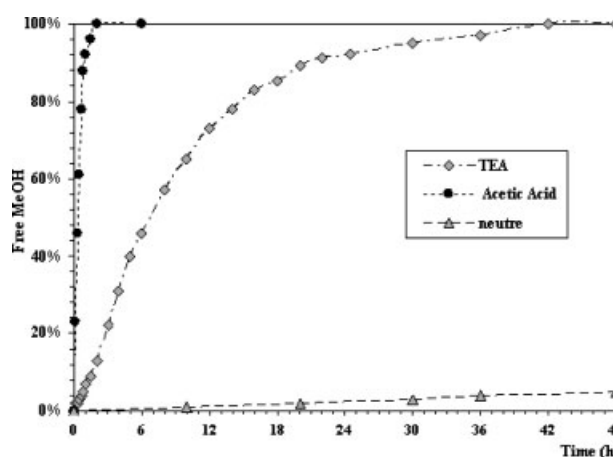


**Figure 1** Evolution of %MeOH released for MRPS at different catalytic conditions.

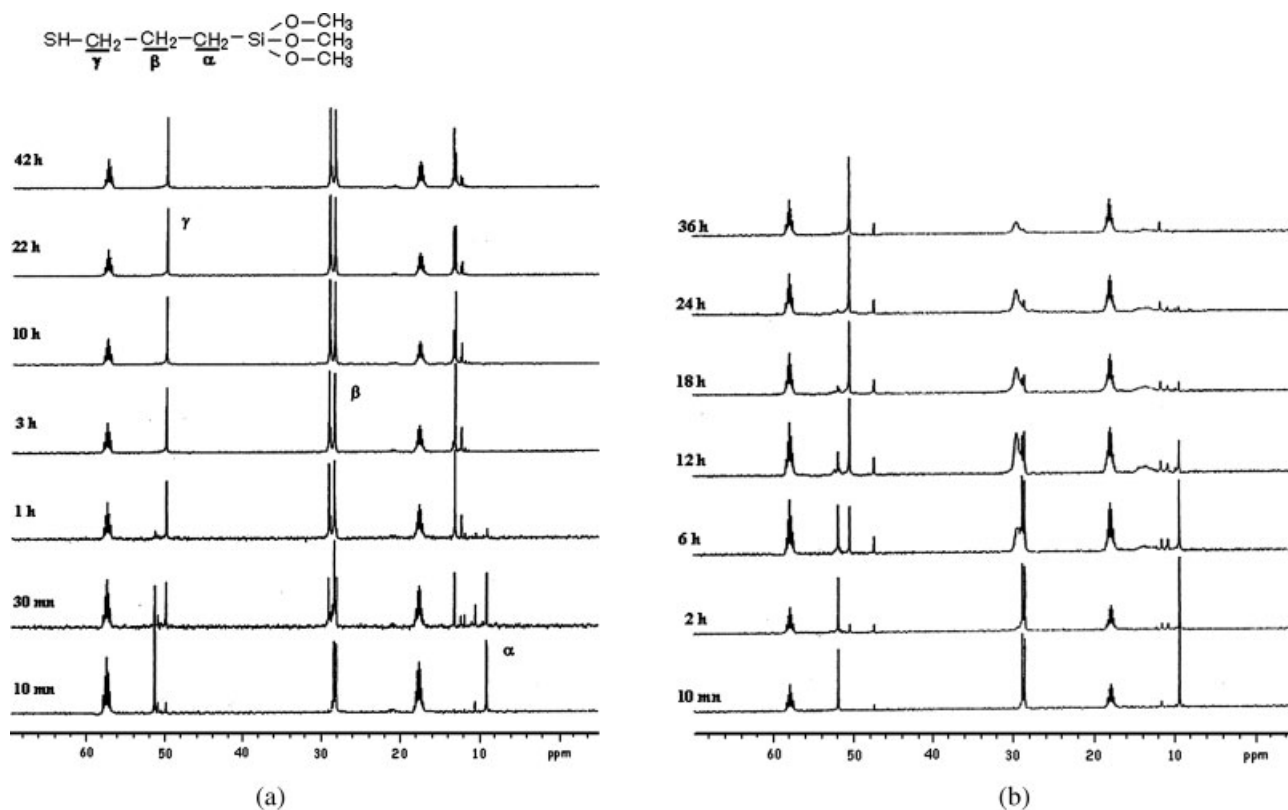


**Figure 2**  $^{13}\text{C}$  NMR spectra under (a) acid and (b) TEA-catalyzed MRPS hydrolysis.

- TEA, some broader peaks are observed, and the S/N decreases drastically with time; after 36-h reaction, the silane is undetectable although the number of scans was greatly increased with time.
- ii. With TEA, the pristine silane  $T_R^0$  decreases with time in agreement with the hydrolysis

rate noticed with  $^1\text{H}$  NMR. No silanol  $T_H^0$  entities could be detected. Before the complete disappearance of the initial MRPS some condensed units  $T^1$ ,  $T^2$ , and  $T^3$  are observed but very quickly the S/N drops down hard fully.

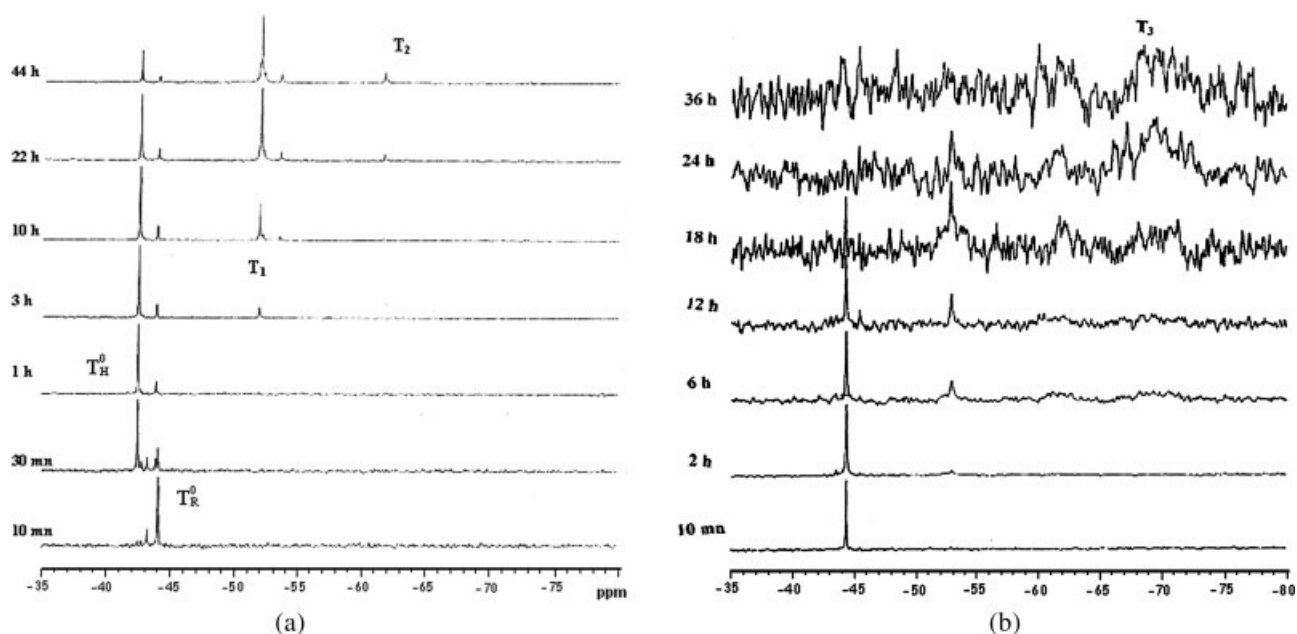


**Figure 3**  $^{29}\text{Si}$  NMR spectra under (a) acid and (b) TEA-catalyzed hydrolysis of MRPS.

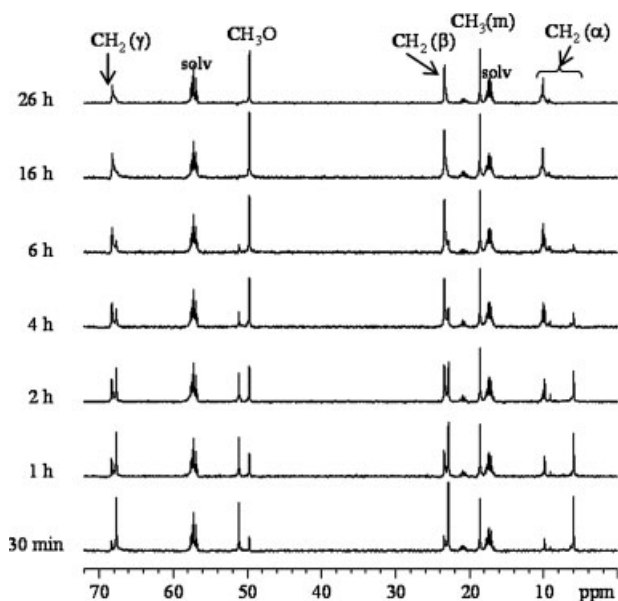


**Figure 4**  $^{13}\text{C}$  NMR spectra of acid-catalysed hydrolysis of MPS.

- iii. In acidic conditions the short lived species  $^{13}\text{C}$  observation is confirmed. The major signal of totally hydrolyzed silanol  $T_H^0$  at  $-41.1$  ppm, and the partially hydrolysed silanol at  $-41.4$  and  $-41.9$  ppm are noticed. The hydrolysed moieties reach more than 95% after 1-h reaction, and then they decrease slowly. It remains more than 50%  $T_H^0$  units after 12-h reaction.
- iv. From the 3rd hour the formation of  $T^1$  units at  $-50.6$  ppm begins and continues to increase slowly till about 70% after 48-h reaction.
- v. The generation of  $T^2$  (representing linear chains only in the absence of  $T^3$  units), at  $-60.2$  ppm, starts after 18 h and pursue with an extremely low rate. It does not exceed 10% after 48 h reaction. No  $T^3$  entities are detected during the experiment time.

In presence of TEA, the hydrolysis is the limitation rate reaction and the very fast condensation reactions lead to the condensed  $T^1$ ,  $T^2$ , and  $T^3$  structure concomitantly to the silanol formation, so the silanol moieties couldn't be detected because of their immediate consummation when they are formed. With the reaction progression three dimensional networks resulting from the growth of condensed  $T^3$  units give rise to colloidal particles that precipitate in the medium and are responsible of the drastic decrease of S/N noticed both in  $^{13}\text{C}$  and in  $^{29}\text{Si}$  NMR. One can also note that NMR resonance relative to  $T^2$  and  $T^3$  units are relatively large suggesting irregular macromolecular structure which is in agreement with  $^{13}\text{C}$  NMR observations.

In acidic medium MRPS hydrolysis is faster and the condensation reactions are drastically slow

down, so the hydrolysed entities are much more stabilized. From 1-h reaction till the end of the observation (48 h) 100% of the entities in solution are graftable with OH-owing surfaces, they bear one or more free Si—OH branch. The major part of these hydrolysed species is dimeric moieties.

Similar trends were noted for MPS. The hydrolysis rates are lower than that of MRPS either in acidic or in basic media (Fig. 1). But without any catalyst, MPS hydrolysis rate is higher than that of MRPS though it remains very low (10% hydrolysis after 24 h).

The general behaviour of these two silanes is similar: with TEA, very broad peaks associated with high molecular weight moieties are noticed on  $^{13}\text{C}$  and  $^{29}\text{Si}$  spectra, then in acidic media very sharp peaks relied with monomeric, dimeric, and low molecular oligomeric structures are observed. Nevertheless some differences could be remarked, as seen in Figures 4 and 5.

With TEA-catalyse hydrolysis the profile of formation of the different silicon moieties is similar for the two silanes.<sup>23</sup> In spite of the preponderant formation of very large high molecular  $T^3$  units no precipitation inducing a S/N decrease is observed with MPS TEA-hydrolysis; the siloxane network remains viscous but liquid even after 1 year.<sup>23,24</sup>

In acidic medium for both two silanes no  $T^3$  entities are detected during the experiment time (48-h observation). After 48-h reaction 100% of the species in solution are graftable, but their formation kinetics are different for MPS and MRPS. Figure 5 shows that the maximum of MPS silanol entities  $T_H^0$ , more than 75%, is obtained after 3- to 4-h reaction (com-

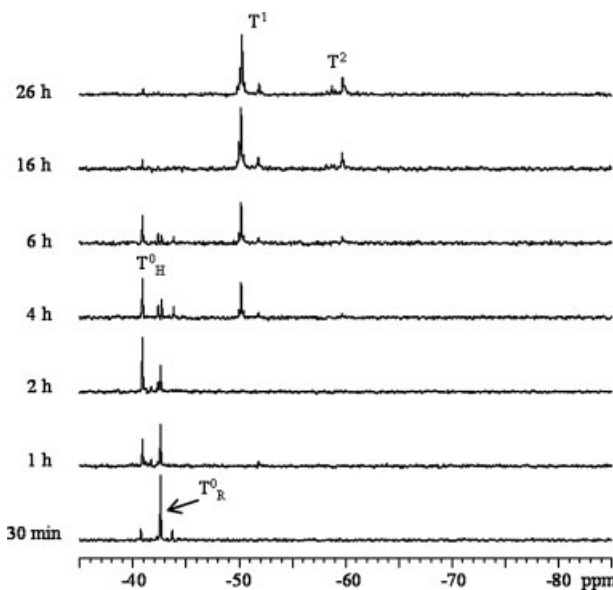


**Figure 5**  $^{29}\text{Si}$  NMR spectra of acid-catalysed hydrolysis of MPS.

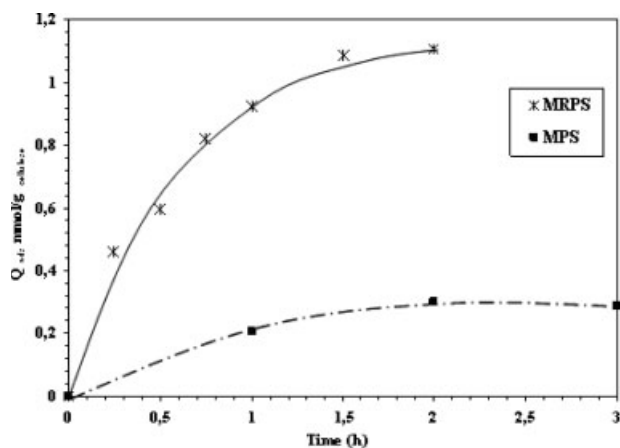


**Figure 6** Evolution of the adsorbed amount of MPS and MRPS on cellulose fibers versus time using a solution having an initial concentration of 0.08 and 0.05 mol/L, respectively.

pared to 95% after 1-h reaction for MRPS). After 12-h reaction there are 50%  $T_H^0$  and 50%  $T^1$  for MPS instead of 60 and 40%, respectively for MRPS. After 24-h reaction moieties in solution are 15%  $T_H^0$ , 75%  $T^1$ , and 10%  $T^2$  for MPS in place of 35, 60, and 5%, respectively for MRPS. At the end of the observation (48-h reaction) it remains 5% initial silanol  $T_H^0$ , 80%  $T^1$ , and 15%  $T^2$  for MPS; and for MRPS 20, 70, and 10%, respectively. The MPS hydrolysis is slower than that of MRPS, but the condensation reactions are slightly faster. So in acidic medium even though 100% of the entities in solution are graftable for both two silanes, the MRPS has higher anchoring possibilities because at every time it bears the higher number of free Si—OH branch for a further OH-surface matrix condensation.

From this set of experiments, one can conclude that the acid-catalyzed hydrolysis of silane allows the formation of high amount of silanol groups, reduced the selfcondensation reaction among silanol

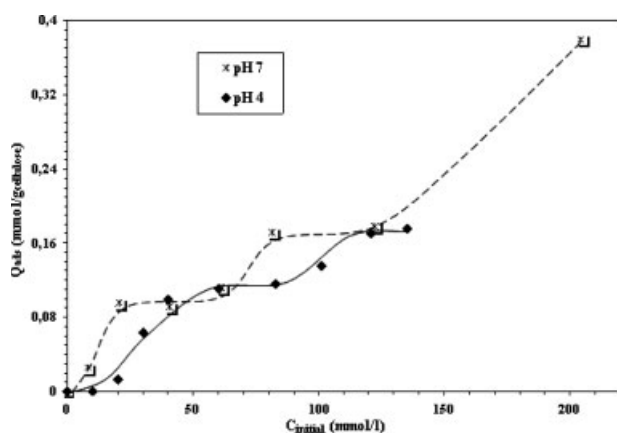


**Figure 7** Adsorption isotherm of MPS on cellulose fibers at two different pH solution.

groups and stabilized the proportion of intermediary hydrolyzed species for several days. On the other hand, under basic condition, condensation reactions proceed as soon as the hydrolysis reaction started leading to the rapid consumption of silanol groups, reaction, through selfcondensation reaction that issue to three-dimensional high molecular structures and impede any NMR. The growth of these structures will greatly affect the chemical anchoring power of these silanes.

### Adsorption isotherms

The second part of our study concerned the adsorption behaviour of MPS and MRPS on cellulose fibers. For all the experiment, the contact time of cellulose suspension with silane solution of 2 h was adopted, to establish the adsorption isotherm. Indeed, as shown in Figure 6 the adsorption amount reached a plateau after 2 h and did not evolve with further contact time. The adsorption isotherms of MPS and MRPS are given in Figures 7 and 8, which show that, under acidic conditions, for both silanes no detectable adsorption was noted, below an initial concentration of 20 mmol L<sup>-1</sup> (corresponding to about 0.5% w/w with respect to cellulose). Then, the adsorption has grown and reached a first plateau at about 0.092 and 0.2 mmol g<sup>-1</sup> for MPS and MRPS, respectively. A second plateau at 0.17 and 0.4 mmol g<sup>-1</sup> has appeared when higher amounts of the added amount of silane solution was achieved (more than 2% w/w).

Under neutral conditions, a continuous increase in the silane adsorption was observed. A single plateau was found for MRPS and a multiple adsorption plateau was encountered for MPS. These results were quite unexpected when compared to those established under acid condition, in which at least 80% of the silanol groups were present, while under neutral

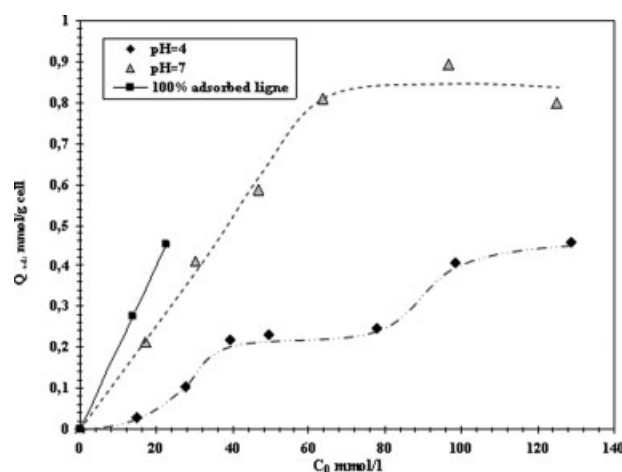


**Figure 8** Adsorption isotherm of MRPS on cellulose fibers at two different pH solution.

condition the silane hydrolysis was practically negligible. Therefore, it can be deduced that the silanol groups  $-\text{Si}-\text{OH}$  are not indispensable to promote adsorption (through hydrogen bonding with hydroxyl groups of cellulose substrate). Thus, the adsorption seems to be driven by van der Waals interactions. Apparently silanol groups display higher affinity toward the continuous ethanol-water medium (high solvation process), which reduced the silane accumulation on the fibre's surface. On the other hand the relatively hydrophobic character of the pristine silane favours its adsorption thanks to the lower interaction possibility among water or ethanol solvent molecules and nonhydrolyzed silane components. This behavior disagrees with that observed for inorganic substrate.<sup>31</sup>

### XPS analysis

XPS analyses were carried out to give qualitative and quantitative evidences of silane presence on the fibre surface. After the silane adsorption, the fibers were submitted to a thermal treatment at  $110^\circ\text{C}$ , in order to bring about chemical binding of the coupling agent to the cellulose surface. XPS is the most adapted technique to provide both qualitative and quantitative information, regarding the different elements present on the surface and their chemical environment, when the quantity of the grafted molecules is too low. Figure 9 depicts XPS survey spectra of electron intensity as a function of binding energy for virgin material, MPS- and MRPS-treated fibers. As expected, pristine cellulose displayed only two peaks at about 533 and 285 eV, attributed to  $\text{O}_{1s}$  and  $\text{C}_{1s}$ , respectively. On the other hand, for silane treated fibers, in addition to the peaks associated with oxygen and carbon, the following peaks were detected: (i) peaks at 103 and 153 eV, characteristics of  $\text{Si}_{2s}$  and  $\text{Si}_{2p}$  respectively, were found for all the treated samples; (ii) peak at 400 eV attributed to nitrogen atoms was detected for PAPS-treated cellulose; and (iii) peak at 165 eV, associated with the presence of S atoms was observed for MRPS-treated fibers. These data confirm the presence covalent bonds between the silanes and the cellulose fibers.

Elemental composition on the surface layer, determined from the area of each peak normalized with sensitivity factors, for different silane modified fibers are summarised in Table III. It is worth to note that the amount of sulphur and nitrogen is close to that of silicon in MRPS and PAPS, as expected from their respective structures. Likewise, the amount of anchored silane varied from 0.8 to 1.5% based on the surface layer. The highest level is observed for OS treated fibers followed by MPS fibers, followed by MRPS (neutral treatment), MRPS (acid treatment) and, finally, PAPS. Considering that, in XPS, the

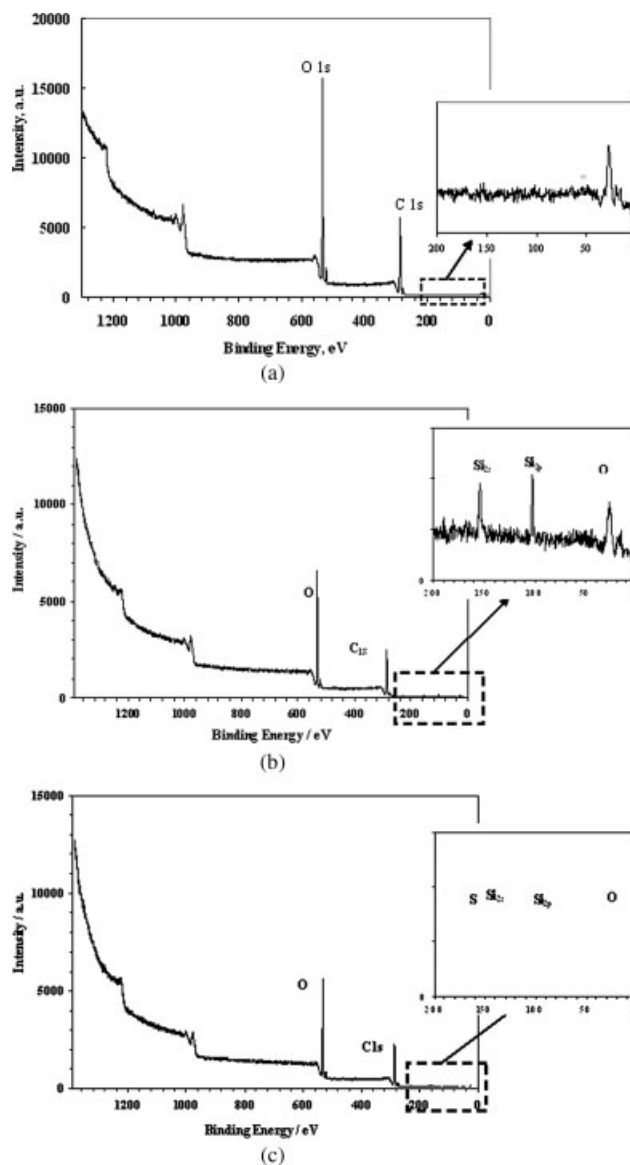


**Figure 9** XPS Spectra of (a) untreated, (b) MPS and (c) MRPS-treated cellulose fibers.

depth of analysis is about 5 nm, and the unit cell dimension of cellulose separating two cellulose plans is about  $8 \text{ \AA}$ ,<sup>32</sup> we could estimate that the surface coverage of silane ranged from 0.6 to 1 silane molecules per anhydroglucosic unit at the surface of cellulose macromolecule.

However, when we analyze the amount of Si anchored on the surface after the thermal treatment a different trend is noted when compared to results arising from adsorption isotherms (Figs. 7 and 8). Indeed, the higher atomic concentration is attained for MPS (acid treatment) followed by MRPS (neutral treatment) and MRPS (acid treatment) while the adsorbed amount for MRPS (neutral treatment) is six times higher than MPS (acid treatment) and four times higher than MRPS (acid treatment) fibers. This discrepancy could be rationalised if one considers



**TABLE III**  
Elemental Quantifications: Atomic Concentrations (%) and Atomic Ratios

	PAPS	MPS, pH = 4	SH, pH = 7	SH, pH = 4	OS
TOA = 90°					
C 1s	58.51	55.99	56.57	59.09	59.63
O 1s	40.05	42.37	41.2	39.24	38.73
N 1s	0.84	0.2	0.21	0.2	
Si 2p	0.61	1.43	1.11	0.83	1.64
S 2p			0.91	0.64	
Atomic ratios					
O/C	0.68	0.76	0.73	0.66	0.65
N/C	0.0144	0.0036	0.0037	0.0034	
Si/C	0.0104	0.0255	0.0196	0.0140	0.0275
S/C			0.0161	0.0108	
TOA = 30°					
C 1s	60.55	58.06	59.01	61.14	61.62
O 1s	38.11	40.06	38.45	36.73	36.36
N 1s	0.7	0.24	0.24	0.33	
Si 2p	0.64	1.65	1.3	1.01	2.03
S 2p			1	0.79	
Atomic ratios					
O/C	0.63	0.69	0.65	0.60	0.59
N/C	0.0116	0.0041	0.0041	0.0054	
Si/C	0.0106	0.0284	0.0220	0.0165	0.0329
S/C			0.0169	0.0129	

that a part of the adsorbed silane was evaporated from the surface during the thermal treatment under partial vacuum. This event is likely to occur since it has already been shown that the pre-hydrolysed silanes are only physically adsorbed on cellulose and it's their chemical anchoring to the surface could not occur only after the thermal treatment.<sup>33</sup> In fact, the lower the hydrolysis and the condensation degree of the adsorbed silane, the higher is the risk of evaporation during the thermal treatment. This could justify why the Si atomic concentration is roughly the same for MRPS-treated fibers arising from neutral and acid hydrolysis. These results provide valuable information about the care to take, in order to ensure efficient anchoring of silane on organic surface bearing hydroxyl groups, in general, and on cellulose substrate in particular. This is of high importance because these surfaces differ from inorganic oxide, namely SiO<sub>2</sub> which does not require any thermal treatment to ensure silane anchoring.

The deconvolution of C<sub>1s</sub>, N<sub>1s</sub>, and Si<sub>2p</sub> peaks gives better information regarding chemical environment of different elements detected on the surface of fibers, as shown in Figure 10. XPS C<sub>1s</sub> peaks were fitted with three components (and four components in the case of MPS), and the ensuing results are summarized in Table IV. The signal of C<sub>1s1</sub>, around 285 eV, is assigned to aliphatic carbons including the contribution of carbons bound to silicon (C—Si) at 284.5 eV. OS-treated cellulose presents a relative high amount of aliphatic carbons compared to the

**TABLE IV**  
Relative Amount of C<sub>1s1</sub>

	PAPS	MPS, pH = 7	SH, pH = 7	SH, pH = 4	OS
C 1s 1/ (C 1s 2+C 1s 3)	0.30	0.26	0.32	0.36	0.50

other silane originating from the octyl moiety of OS. The increase in C<sub>1</sub> contribution after treatment indicates the anchoring of silane on cellulose surface, since its presence enriches this signal by three aliphatic carbons. The binding energy of the most intense component, C<sub>1s2</sub>, was taken as the reference to correct the charge shifts. It is centred at 286.73 eV and is attributed to —C—OH and —C—O— of cellulose<sup>34,35</sup> (as shown in Scheme 2). C<sub>1s3</sub> corresponds to O—C—O of cellulose (Carbon "2" in Scheme 2). The fourth component at 289.3 eV appeared only on MPS treated. It is assigned to O—C=O rising from methacrylate function. The binding energy of Si 2<sub>p1</sub> (Si 2p<sub>3/2</sub>), 102.5 ± 0.2 eV, is typical of silicon in si-

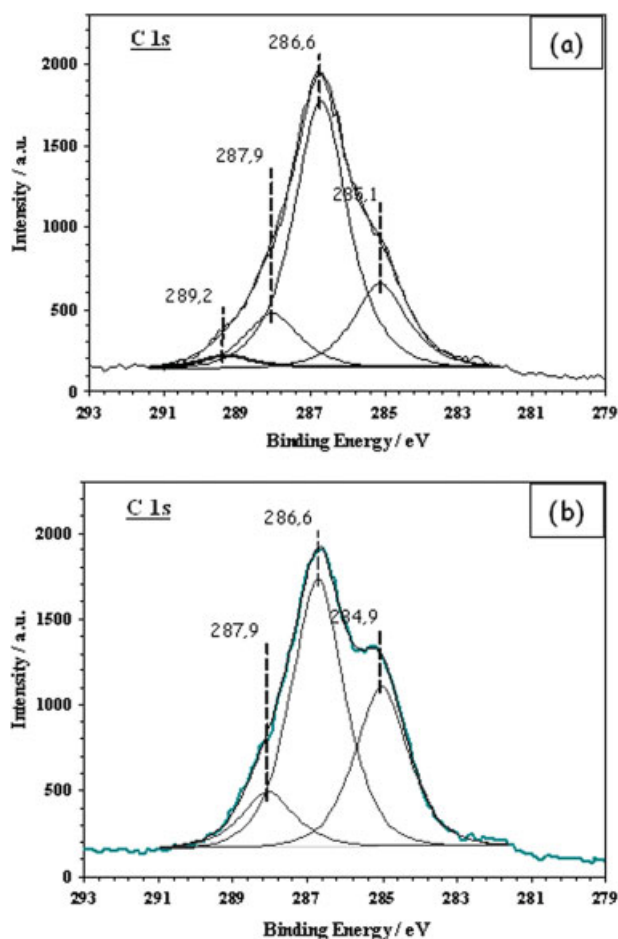


**Figure 10** Deconvolution of C<sub>1s</sub> peak of XPS Spectra of (a) MRPS and (b) OS-treated cellulose fibers. [Color figure can be viewed in the online issue, which is available at [www.interscience.wiley.com](http://www.interscience.wiley.com).]

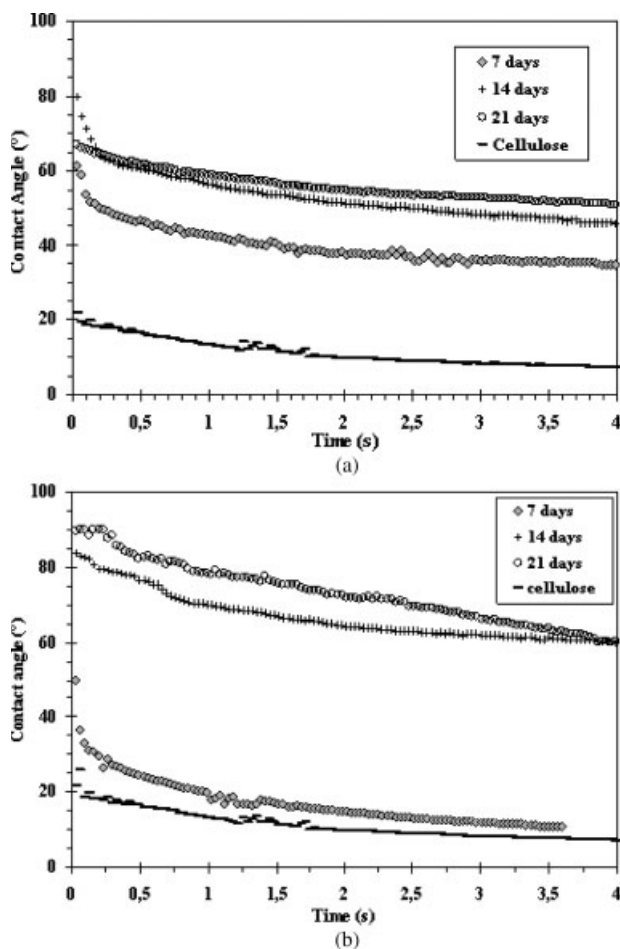


**Figure 11** Water contact angle evolution of (a) MRPS, and (b)MPS –modified cellulosic fibers treated under pH 4 as a function of drying time after heat treatment.

loxane groups. The content in Silicon atoms follows the same trend than that of O/C ratio, for the different treated fibers.

O<sub>1s</sub> was fitted with two components and the ensuing signals assigned to cellulose oxygen atoms: O<sub>1s1</sub>, around 533 eV was attributed to oxygen in hydroxyl groups and O<sub>1s2</sub>, around 533.6 eV was associated to O–C–O (a–b). Furthermore, the difference B.E.(O<sub>1s1</sub>) – B.E.(O<sub>1s2</sub>) = 246.2 ± 0.1 eV is typical of –C–OH bonds in cellulose. Moreover, the quantitative analysis shows that the oxygen present in these samples is not exclusively from cellulose. All samples present a ratio (O<sub>1s1</sub> + O<sub>1s2</sub>)/(C<sub>1s2</sub> + C<sub>1s3</sub>) larger than the theoretical value O/C in cellulose unit (0.83), indicating that oxygen originates also come from anchored silane on the surface.

**Contact angle analysis**

The evolution of the contact angle values of a drop of water deposited on the WH5 sheets after their treatment with various coupling agents and at different

conditions is shown in Figures 11–13. As expected, in the absence of silane the virgin fibers display a low contact angle (near to 20°) arising from the presence of a high density of hydroxyl groups on cellulose backbone. Treatment with silane brings about an increase in the contact angle. However, the evolution depends on many parameters such as the pH, the delay between the thermal treatment and the adsorption procedure and the silane structure. When the adsorption is carried in presence of acetic acid (Figs. 11 and 12), the contact angle after the thermal treatment both for MRPS and MPS did not attain a constant value only after ageing of the fibers at ambient condition for 14 days. Above this delay the contact angle attained about 70° and 80° for MRPS and MPS, respectively. This effect was much less pronounced when adsorption occurred under neutral condition.

When the silane is previously adsorbed from neutral solution the effect of the delay period seems to be less pronounced. The higher reactivity of the

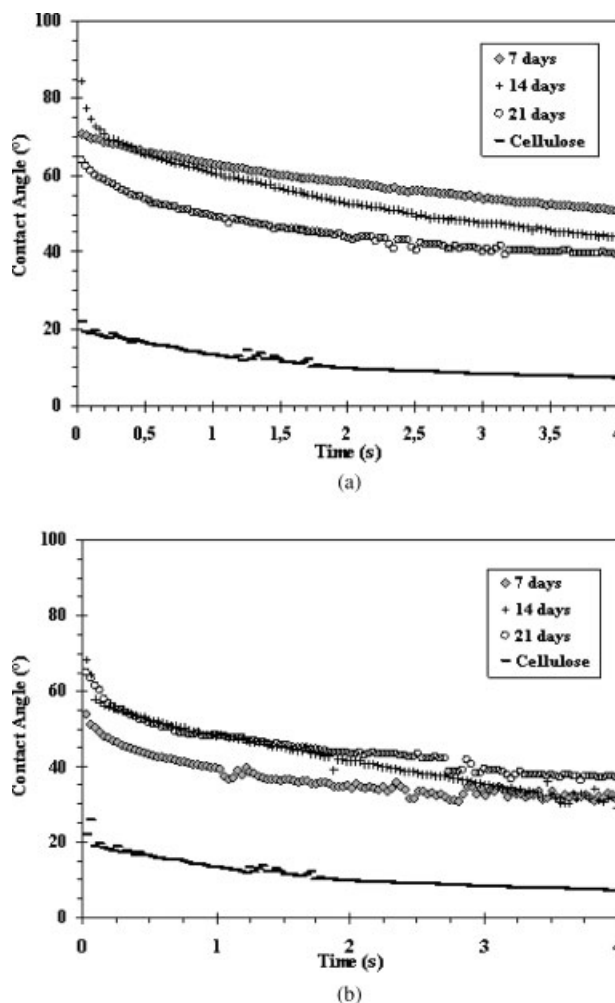


**Figure 12** Water contact angle evolution of (a) MRPS, and (b) MPS –modified cellulosic fibers treated under pH 7 as a function of drying time after heat treatment.

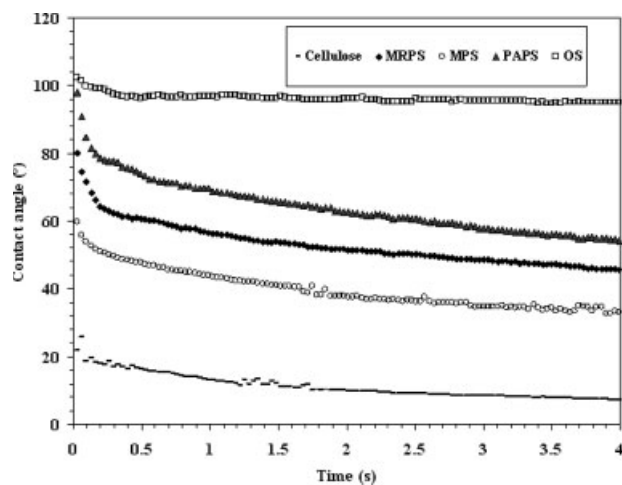


**Figure 13** Water contact angle as a function of the silane structure after heat treatment. (adsorption under pH 4, drying time 21 days).

methoxysilane toward condensation may account for this behaviour. In this case selfcondensation occurred between methoxy or ethoxysilane and silanol ends arising from partial hydrolysis of methoxysilane by atmospheric humidity. However, the presence of free non hydrolysed silane on the surface may lead to some loss either while the sample is exposed to the ambient atmosphere or by evaporation during the thermal treatment. The evolution of the contact angle versus the silane structure, depicted in Figure 13 showed that for trialkoxy silane, the contact angle varies according to the following trend; OS > PAPS > MRPS > MPS. This trend is in agreement with the relative hydrophobic character of the radical alkyl appended to the silicon atom.

## CONCLUSIONS

The hydrolysis of silanes under acidic catalysis yielded the formation of high amount of silanol groups and reduced the selfcondensation reaction of the ensuing reactive silanol groups.

The silane adsorption on the cellulose fibers was greatly affected by the pH. It infer that the hydrolysis of the silane giving rise to silanol groups is not necessary to promote the adsorption, which seems to be driven by van der Waals interactions with cellulose fibers rather than hydrogen bonding of silanol with hydroxyl groups of cellulose substrate.

This work should be extended to other silane, to establish the most suitable conditions favouring the formation of monomeric and dimeric hydrolysed species, in order to enhance the probability of silane anchoring on cellulose substrate.

The authors thank Pr. Ana Maria Botelho do Rego and Dr. Anna Maria Ferrara (CQFM-IST) for her help with the XPS measurements.

## References

1. Plueddemann, E. P. *Silane Coupling Agents*; Plenum: New York, 1991.
2. Kim, J. K.; Mai, Y. W. *Engineered Interfaces in Fiber Reinforced Composites*; Elsevier: Oxford, UK, 1998.
3. Kim, J. K.; Mai, Y. W. In *Structure and Properties of Composites*; Chou, T. W., Ed.; VCH: Weinheim, 1993; p 13.
4. Walker, P. J. *Adhes Sci Technol* 1991, 4, 279.
5. Mittal, K. L. *Silanes and Other Coupling Agents*; JSP: Utrecht, 1992.
6. Weaver, K.; Stoffer, J. O.; Day, E. D. *Polym Compos* 1995, 16, 161.
7. Miller, A. C.; Knowlton, M. T.; Berg, J. C. *J Adhes Sci Technol* 2000, 14, 1471.
8. Hoh, K. P.; Ishida, H.; Koenig, J. L. *Polym Compos* 1988, 9, 151.
9. Schmidt, H.; Seifering, B.; Philipp, G.; Deichman, K.; Mackenzie, J. D.; Utrich, D. R. *Ultrastructure Processing of Advanced Ceramic*; Wiley: New York, 1988.
10. Papirer, E.; Balard, H. *J Adhes Sci Technol* 1990, 8, 653.
11. Chu, C. W.; Kirby, D. P.; Murphy, P. D. *J Adhes Sci Technol* 1993, 7, 417.
12. Daniels, M. W.; Francis, L. F. *J Colloid Interface Sci* 1998, 191, 205.
13. Crandall, J. K.; Morel-Fourrier, C. *J Organomet Chem* 1995, 5, 489.
14. Kang, H. J.; Meesiri, W.; Blum, F. D. *Mater Sci Eng A* 1990, 126, 773.
15. Pianna, K.; Schubert, U. *Chem Mater* 1994, 6, 1504.
16. Chiang, C. H.; Ishida, H.; Koenig, J. L. *J Colloid Interface Sci* 1980, 74, 396.
17. Ishida, H.; Koenig, J. L. *Appl Spectrosc* 1978, 32, 469.
18. Riegel, B.; Blittersdorf, S.; Kiefer, W.; Hofacker, S.; Müller, M.; Schottner, G. *J Non-Cryst Solids* 1998, 226, 76.
19. Beari, F.; Brand, M.; Jenkner, P.; Lehnert, R.; Metternich, H. J.; Monkiewicz, J.; Siesler, H. W. *J Organomet Chem* 2001, 208, 625.
20. Daniels, M. W.; Sefcik, J.; Francis, L. F.; McCormick, A. V. *J Colloid Interface Sci* 1999, 219, 351.
21. Nishiyama, N.; Asakura, T.; Horie, N. *J Colloid Interface Sci* 1988, 14, 124.
22. Shin, P. T. K.; Koenig, J. L. *Mater Sci Eng* 1975, 20, 137.
23. Brochier Salon, M. C.; Abdelmouleh, M.; Boufi, S.; Belgacem Mohamed, N.; Gandini, A. *J Colloid Interface Sci* 2005, 289, 249.
24. Brochier Salon, M. C.; Abdelmouleh, M.; Gerbaud, G.; Bruzzese, C.; Boufi, S.; Belgacem, M. N. *Magn Reson Chem* 2007, 45, 473.
25. Abdelmouleh, M.; Boufi, S.; Belgacem, M. N.; Dufresne, A.; Gandini, A. *J Appl Polym Sci* 2005, 98, 974.
26. Abdelmouleh, M.; Boufi, S.; Belgacem, M. N.; Dufresne, A. *Comp Sci Technol* 2007, 67, 1627.
27. Abdelmouleh, M.; Boufi, S.; Belgacem, M. N.; Duarte, A. P.; Ben Salah, A.; Gandini, A. *Int J Adhes Adhes* 2004, 24, 43.
28. Ellman, G. L. *Arch Biochem Biophys* 1959, 82, 70.
29. Riddles, P. W.; Blakeley, R. L.; Zerner Anal Biochem 1979, 94, 75.
30. Glasser, R. H.; Wilkes, G. L. *Polym Bull* 1988, 19, 51.
31. Waddell, T. G.; Leyden, D. E.; DeBello, M. T. *J Am Chem Soc* 1981, 103, 5303.
32. Zugenmaier, P. *Prog Polym Sci* 2001, 26, 1341.
33. Abdelmouleh, M.; Boufi, S.; Ben Salah, A.; Belgacem, M. N.; Gandini, A. *Langmuir* 2002, 3203, 18.
34. Powell, W.; Rumble, C. J. J. R., Jr. *NIST X-ray Photoelectron Spectroscopy Database, NIST Standard Reference Database 20, Version 3.3 (Web Version)*, 2003.
35. Beamson, G.; Briggs, D. *High Resolution XPS of Organic Polymers: The Scienta ESCA300 Database*; Wiley: Chichester, 1992.